Diffusion-Thermo and Thermal Radiation of an Optically Thick Gray Gas in Presence of Magnetic Field and Porous Medium

B. C. Sarkar[1], R. N. Jana[1] and S. Das[2†]

[1]*Department of Applied Mathematics, Vidyasagar University, Midnapore 721 102, India*
[2]*Department of Mathematics, University of Gour Banga, Malda 732 103, India*

†*Corresponding Author Email: tutusanasd@yahoo.co.in*

ABSTRACT

Diffusion-thermo and thermal radiation effects on an unsteady magnetohydrodynamic (MHD) free convective flow past a moving infinite vertical plate with the variable temperature and concentration in the presence of transverse applied magnetic field embedded in a porous medium have been analyzed. The flow is governed due to the impulsive as well as accelerated motion of the plate. The governing equations have been solved by employing the Laplace transform technique. The influences of the pertinent parameters on the velocity field, temperature distribution, concentration of the fluid, shear stress, rate of heat and mass transfers at the plate have been presented either graphically or in tabular form.

Keywords: Magnetohydrodynamic (MHD) flow; Impulsive and accelerated motion; Radiation; Diffusion porous medium.

1. INTRODUCTION

The chemical reaction rate depends on the concentration of the species itself. In many chemical engineering processes, there is the chemical reaction between a foreign mass and the fluid. These processes take place in many industrial applications such as food processing, manufacturing of ceramics and polymer production. The applications of hydromagnetic incompressible viscous flow in science and engineering involving heat and mass transfer under the influence of chemical reaction are of great importance to many areas of science and engineering. The study of MHD flow with heat and mass transfer plays an important role in biological Sciences. Effects of various parameters on human body can be studied and appropriate suggestions can be given to the persons working in hazardous areas having noticeable effects of magnetism and heat variation. Convective heat transfer in porous media has been a subject of great interest for the last few decades. This interest was motivated by numerous thermal engineering applications in various disciplines, such as geophysical, thermal and insulation engineering, the modeling of packed sphere beds, chemical catalytic reactors, the cooling of electronic systems, grain storage, devices fiber and granular insulation, missiles, combustion and furnace design, petroleum reservoirs, coal combustors, ground water pollution and filtration processes. Fourier's law describes the relation between energy flux and temperature gradient and Fick's law determines the relation between mass flux and concentration gradient. The energy flux caused by a composition gradient is called the Dufour or diffusion-thermo effect. This effect is found to be of order of considerable magnitude such that it cannot be neglected.

Gupta *et al*. (1979) have studied the free convective effects on the flow past an accelerated vertical plate in an incompressible dissipative fluid. Jana and Datta (1982) have investigated an unsteady free convective flow past a moving vertical plate. Free convective flow past an exponentially accelerated vertical plate has been described by Singh and Kumar (1984) and Hossain and Shayo (1986). MHD thermal-diffusion effects on free convective mass transfer flow over an infinitely long vertical moving plate have been studied by Kafoussias (1992). Hossain and Takhar (1996) have investigated the radiation effect on mixed convective flow past an infinitely long vertical plate with an uniform surface temperature. Das *et al*. (1996) and Raptis and Perdikis (1999) have presented the radiative free convective flow past an infinitely long moving vertical plate. Muthucumaraswamy and Vijayalakshmi (2005) have described the radiation effects on the flow past an impulsively started vertical plate with variable temperature and mass flux. Alam and Rahman (2006) have discussed Dufour and Soret effects on mixed convection flow past a vertical porous flat

plate with variable suction. Alam *et al*. (2006a), (2006b) have studied the Dufour and Soret effects on MHD free convection and mass transfer flow past a vertical porous plate in a porous medium. They have discussed both the steady and unsteady cases. Diffusion-thermo and thermal-diffusion effects on free convective heat and mass transfer flow in a porous medium with time dependent temperature and concentration have been investigated by Alam *et al*. (2007). Manna *et al*. (2007) have studied an unsteady viscous flow past a flat plate in a rotating system. Thermal radiation effect on a transient MHD flow with mass transfer past an impulsively started vertical plate has been described by Alam and Sarmah (2009). Rajesh and Varma (2009) have presented the radiation and mass transfer effects on an MHD free convective flow past an exponentially accelerated vertical plate with variable temperature. Muthucumaraswamy *et al*. (2009) have studied an unsteady flow past an accelerated infinitely long vertical plate with variable temperature and uniform mass diffusion. Muthucumaraswamy *et al*. (2009) have also discussed the heat and mass transfer on the flow past an accelerated vertical plate with variable mass diffusion. Jha and Ajibade (2009) have investigated the diffusion-thermo effects on free convective heat and mass transfer flow in a vertical channel with symmetric boundary conditions. The combined effects of heat and mass transfer by mixed convective MHD flow past a porous plate with chemical reaction in the presence of heat source have been described by Ahamed and Zueco (2010). Rajesh and Varma (2010) have investigated the radiation effects on an MHD flow through a porous medium with variable temperature or variable mass diffusion. Makinde (2010) has discussed an MHD heat and mass transfer over a moving vertical plate with a convective surface boundary condition. The effects of thermal radiation on an MHD free convective flow past an infinitely long vertical porous plate have been studied by Seethamahalakshmi *et al*. (2011). Vijaya and Verma (2011) have described the radiation effects on an MHD flow past an impulsively started exponentially accelerated vertical plate with variable temperature. Radiation and Darcy effects on an unsteady MHD heat and mass transfer flow of a chemically reacting fluid past an impulsively started vertical plate have been investigated by Suneetha and Bhaskar (2011). Effects of radiation and heat transfer on the flow past an exponentially accelerated vertical plate have been studied by Mandal *et al*. (2011). Das *et al*. (2011) have presented the radiation effect on natural convection past a vertical plate embedded in porous medium with ramped wall temperature. Makinde (2011) has studied an MHD mixed-convection interaction with thermal radiation and chemical reaction past a vertical porous plate embedded in a porous medium. Pattnaik *et al*. (2012) have described the radiation and mass transfer effects on an MHD free convective flow through porous medium past an exponentially accelerated vertical plate with variable temperature. Radiation effects on an MHD flow past an impulsively started vertical plate with variable heat and mass transfer have been

investigated by Rajput and Kumar (2012). Jana *et al*. (2012) have discussed the radiation effects on an unsteady MHD free convective flow past an exponentially accelerated vertical plate with viscous and Joule dissipations on taking into account. Makinde (2012) has analysed a chemically reacting hydromagnetic unsteady flow of a radiating fluid past a vertical plate with constant heat flux. Soret and radiation effects on transient MHD free convection from an impulsively started infinite vertical plate have been investigated by Ahmed (2012). Kishore *et al*. (2013) have studied the effects of radiation and chemical reaction on an unsteady MHD free convective flow of a viscous fluid past an exponentially accelerated vertical plate. Diffusion-thermo and radiation effects on an unsteady MHD flow past an impulsively started infinitely long vertical plate embedded in porous medium with variable temperature and mass diffusion have been investigated by Prakash *et al*. (2013). Chandrakala and Bhaskar (2014) have studied the radiation effects on an MHD flow past an impulsively started infinite vertical plate with mass diffusion. Diffusion-thermo and thermal-diffusion effects on MHD visco-elastic fluid flow past a vertical plate have been analysed by Yasmin *et al*. (2014). Recently, Ibrahim *et al*. (2015). have investigated the radiation and mass transfer effects on MHD oscillatory flow in a channel filled with porous medium in the presence of chemical reaction.

The aim of the present paper is to study the combined effects of diffusion-thermo and thermal radiation on an unsteady MHD free convective flow of a viscous incompressible electrically conducting fluid past a moving vertical plate embedded in porous medium with variable temperature and concentration. It is considered that the fluid to be optically thick instead of optically thin in this problem. Rosseland diffusion approximation is used to describe the radiative heat flux in the energy equation. The dimensionless governing equations are solved by using the Laplace transform technique. The solutions are in terms of exponential, error function and complementary error function form. The effects of pertinent parameters on the fluid velocity, temperature and mass concentration are discussed with the help of graphs and tables.

2. FORMULATION OF THE PROBLEM AND ITS SOLUTION

Consider an unsteady MHD free convective flow of a viscous incompressible electrically conducting radiating fluid past an infinitely long vertical plate with variable temperature and mass diffusion embedded in a porous medium. The chemical reaction is taking place in the flow. The convection current is induced due to both the temperature and concentration differences. Choose a cartesian co-ordinates system with the x - axis is taken along the plate in the vertically upward direction and the y - axis is normal to the plate in the fluid [See Fig.1]. Initially, at time $t \leq 0$, both the plate and the fluid

are assumed to be at the same temperature T_∞ with concentration level C_∞. At time $t > 0$, the plate at $y = 0$ starts to move in its own plane with a velocity $U_0(t)$, the temperature of the plate and the concentration level are raised to $T_\infty + (T_w - T_\infty)\dfrac{t}{t_0}$ and $C_\infty + (C_w - C_\infty)\dfrac{t}{t_0}$ respectively, T_w being the temperature of the plate, C_w the concentration of the fluid near the plate and t_0 being a constant. A uniform transverse magnetic field of strength B_0 is imposed perpendicular to the plate. The fluid considered here is a gray, absorbing/emitting radiation, but a non-scattering medium. It is assumed that a radiative heat flux q_r is applied in the normal direction to the plate. In the governing equations, the temperature is influenced by concentration leading to diffusion-thermo (Dufour) effect on the heat and mass transfer. The Dufour effect is described by a second-order concentration derivative with respect to the transverse co-ordinate in the energy conservation equation. As the plate is infinitely long, the velocity, temperature and concentration distributions are functions of y and t only.
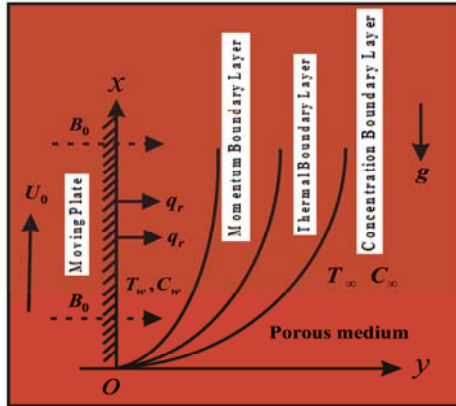

Fig. 1. Geometry of the problem.

Ohm's law is

$$\vec{J} = \sigma\left[\vec{E} + \vec{q} \times \vec{B}\right], \tag{1}$$

where $\vec{J}$ is the current density vector, $\vec{E} \equiv (E_x, E_y, E_z)$ the electric field vector, $\vec{q} \equiv (u, 0, 0)$ the fluid velocity vector and $\vec{B}$ the the magnetic field vector. It is assumed that induced magnetic field produced by the fluid motion is negligible in comparison with the applied one so that we consider magnetic field $\vec{B} \equiv (0, B_0, 0)$. This assumption is justified, since the magnetic Reynolds number is very small for metallic liquids and partially ionized fluids (Cramer and Pai, 1973). The conservation of electric current

$\nabla \bullet \vec{J} = 0$ yields $j_y =$ constant where $\vec{J} \equiv (j_x, j_y, j_z)$. This constant is zero since $j_y = 0$ at the plate which is electrically non-conducting. Hence, $j_y = 0$ everywhere in the flow. As the induced magnetic field is neglected, Maxwell's equation $\nabla \times \vec{E} = -\dfrac{\partial \vec{B}}{\partial t}$ becomes $\nabla \times \vec{E} = \vec{0}$ which gives $\dfrac{\partial E_x}{\partial y} = 0$ and $\dfrac{\partial E_z}{\partial y} = 0$. This implies that $E_x =$ constant and $E_z =$ constant everywhere in the flow.

In view of the above assumption, Eq. (1) yields

$$j_x = \sigma E_x, \tag{2}$$

$$j_y = \sigma E_y = 0, \tag{3}$$

$$j_z = \sigma(E_z + u B_0). \tag{4}$$

As, $y \to \infty$ $j_x \to 0$, $j_z \to 0$, since the magnetic field is uniform at infinity. Using these conditions, equations (2)-(4) give $E_x = E_y = E_z = 0$ everywhere in the flow. Hence from (2) and (4) we have

$$j_x = 0, \tag{5}$$

$$j_z = \sigma B_0 u. \tag{6}$$

With above assumptions the magnetic body force $\vec{J} \times \vec{B}$ reduces simply to $-\sigma B_0^2 u$. .

On the use of (5) and (6), by employing Boussinesq approximation, making use of the standard boundary layer approximations and eliminating pressure the momentum, energy and mass concentration equations in the presence of magnetic field and thermal radiation can be expressed as

$$\frac{\partial u}{\partial t} = \nu \frac{\partial^2 u}{\partial y^2} + g\beta(T - T_\infty) + g\beta^*(C - C_\infty)$$
$$- \frac{\sigma B_0^2}{\rho}u - \frac{\nu}{k^*}u, \tag{7}$$

$$\rho c_p \frac{\partial T}{\partial t} = k\frac{\partial^2 T}{\partial y^2} - \frac{\partial q_r}{\partial y} + \frac{\rho D_m K_T}{C_s}\frac{\partial^2 C}{\partial y^2}, \tag{8}$$

$$\frac{\partial C}{\partial t} = D\frac{\partial^2 C}{\partial y^2} - k_r(C - C_\infty), \tag{9}$$

where u is the velocity in the x-direction, T the temperature of the fluid, C the concentration in the fluid, D the mass diffusivity, D_m the coefficient of mass diffusivity, t the time, g the acceleration due to gravity, ν the kinematic viscosity, ρ the fluid density, β the thermal expansion coefficient, β^* the concentration expansion coefficient, c_p the specific heat at constant pressure, C_s the concentration susceptibility, k the thermal

conductivity, k^* the permeability of the porous medium, K_T the thermal diffusion ratio, k_r the reaction rate constant and q_r the radiative heat flux. For small velocities, the heat due to viscous dissipation is neglected in energy Eq. (8).

In many transport process in nature, flow is driven by density differences caused by temperature gradient, chemical composition (concentration) gradient and material composition. It is therefore important to study flow induced by concentration differences independently or simultaneously with temperature differences. The energy flux caused by the composition gradient is called the Dufour effect (diffusion-thermo). If, on other hand, mass fluxes are created by temperature gradients, it is called the Soret effect (thermal-diffusion). These effects are generally of a small order of magnitude. The Soret and Dufour effects have been found to be of importance as the Soret effect is utilized for isotope separation and, in a mixture of gases of light molecular (H_2, He) and medium molecular weight (N_2, air), the Dufour effect was found to be of an order of magnitude such that it cannot be neglected. The concentration of the species at the plate surface is higher than the solubility of species in the fluid far away from the plate i.e. free stream concentration.

The initial and boundary conditions are

$$t \leq 0 : u = 0, \ T = T_\infty, \ C = C_\infty \ \text{ for all } \ y \geq 0,$$

$$t > 0 : u = U_0(t), \ T = T_\infty + \left(T_w - T_\infty\right)\frac{t}{t_0},$$

$$C = C_\infty + \left(C_w - C_\infty\right)\frac{t}{t_0} \ \text{ at } \ y = 0 \qquad (10)$$

$$t > 0 : u \to 0, \ T \to T_\infty, \ C \to C_\infty \ \text{ as } \ y \to \infty.$$

The radiative heat flux can be found from Rosseland approximation (Siegel and Howell (2002)) and its formula is derived from the diffusion concept of radiative heat transfer in the following way

$$q_r = -\frac{4\sigma^*}{3k_R}\frac{\partial T^4}{\partial y}, \qquad (11)$$

where σ^* is the Stefan-Boltzman constant and k_R the Rosseland mean absorption coefficient of the medium. It should be noted that by using the Rosseland approximation the present analysis is limited to optically thick fluids. It is assumed that the fluid is an optically thick (photon mean free path is very small) gray gas (which emits and absorbs but does not scatter thermal radiation). In an optically thick medium the radiation penetration length is small compare to the characteristic length. The photon mean path is the average distance travelled by a moving photon between successive collisions which modify its direction or energy or other particle properties. If the temperature difference within the flow is sufficiently small, then the Eq. (11) can be linearized by expanding T^4 into

the Taylor series about T_∞ as follows:

$$T^4 = T_\infty^4 + 3T_\infty^3(T - T_\infty) + 6T_\infty^2(T - T_\infty)^2 + \cdots \qquad (12)$$

from which neglecting higher order terms to give

$$T^4 = 4T_\infty^3 T - 3T_\infty^4. \qquad (13)$$

In view of (5) and (7), Eq. (2) becomes

$$\rho c_p \frac{\partial T}{\partial t} = k\frac{\partial^2 T}{\partial y^2} + \frac{16\sigma^* T_\infty^3}{3k_R}\frac{\partial^2 T}{\partial y^2} + \frac{\rho D_m K_T}{C_s}\frac{\partial^2 C}{\partial y^2}. \qquad (14)$$

Introducing non-dimensional variables

$$\eta = \frac{y u_0}{\nu}, \tau = \frac{t}{t_0}, t_0 = \frac{\nu}{u_0^2}, u_1 = \frac{u}{u_0},$$

$$U_0(t) = u_0 f(\tau), \ \theta = \frac{T - T_\infty}{T_w - T_\infty}, \ \phi = \frac{C - C_\infty}{C_w - C_\infty}, \qquad (15)$$

Eqs. (7), (14) and (9) become

$$\frac{\partial u_1}{\partial \tau} = \frac{\partial^2 u_1}{\partial \eta^2} + Gr\theta + Gc\phi - M^2 u_1 - \frac{u_1}{Da}, \qquad (16)$$

$$\frac{\partial \theta}{\partial \tau} = \frac{1}{Pr}\left(1 + \frac{4}{3R}\right)\frac{\partial^2 \theta}{\partial \eta^2} + Du\frac{\partial^2 \phi}{\partial \eta^2}, \qquad (17)$$

$$Sc\frac{\partial \phi}{\partial \tau} = \frac{\partial^2 \phi}{\partial \eta^2} - K\phi, \qquad (18)$$

where $M^2 = \frac{\sigma B_0^2 \nu}{\rho u_0^2}$ is the magnetic parameter, $R = \frac{k k_R}{4\sigma^* T_\infty^3}$ the radiation parameter, $Pr = \frac{\rho \nu c_p}{k}$ the Prandtl number, $Gr = \frac{g\beta(T_w - T_\infty)\nu}{u_0^3}$ the thermal Grashof number, $Gc = \frac{g\beta^*(C_w - C_\infty)\nu}{u_0^3}$ the mass Grashof number, $Sc = \frac{\nu}{D}$ Schmidt number, $Da = \frac{u_0^2 k^*}{\nu^2}$ the porosity parameter, $K = \frac{k_r \nu^2}{D u_0^2}$ the chemical reaction parameter and $Du = \frac{D_m K_T}{C_s c_p \nu}\frac{C_w - C_\infty}{T_w - T_\infty}$ the Dufour number. In Eq. (17), the non-zero value of Dufour number physically represents that the temperature distribution is affected by concentration gradient. For $Du = 0$, Eq. (17) reduces to the classical energy equation obeying Fourier's law of heat conduction.

The initial and boundary conditions for u_1, ϕ and θ are

$$t \leq 0 : u_1 = 0, \ \phi = 0, \ \theta = 0 \ \text{ for all } \ \eta \geq 0,$$

$$t > 0 : u_1 = f(\tau), \ \phi = \tau, \ \theta = \tau \ \text{ at } \ \eta = 0, \qquad (19)$$

$t > 0 : u_1 \to 0, \ \phi \to 0, \ \theta \to 0 \ \text{as} \ \eta \to \infty.$

On the use of the Laplace transformation, Eqs. (16) - (18) become

$$\left(s + M^2 + \frac{1}{Da}\right)\bar{u}_1 = \frac{d^2\bar{u}_1}{d\eta^2} + Gr\,\bar{\theta} + Gc\,\bar{\phi}, \tag{20}$$

$$s\bar{\theta} = \frac{1}{Pr}\left(1 + \frac{4}{3R}\right)\frac{d^2\bar{\theta}}{d\eta^2} + Du\frac{d^2\bar{\phi}}{d\eta^2}, \tag{21}$$

$$s\,Sc\,\bar{\phi} = \frac{d^2\bar{\phi}}{d\eta^2} - K\bar{\phi}, \tag{22}$$

$$\bar{u}_1(\eta,s) = \int_0^\infty u_1(\eta,\tau)e^{-s\tau}\,d\tau, \ \ \bar{\theta}(\eta,s) = \int_0^\infty \theta(\eta,\tau)e^{-s\tau}\,d\tau \ \text{a}$$

nd

The corresponding boundary conditions for $\bar{u}_1$, $\bar{\phi}$ and $\bar{\theta}$ are

$$\bar{u}_1 = f(s), \ \bar{\phi} = \frac{1}{s^2}, \ \bar{\theta} = \frac{1}{s^2} \ \text{at} \ \eta = 0,$$

$$\bar{u}_1 \to 0, \ \bar{\phi} \to 0, \ \bar{\theta} \to 0 \ \text{as} \ \eta \to \infty. \tag{24}$$

Solutions of Eqs. (20)-(22) subject to the boundary conditions (24) are easily obtained and are given by

$$\bar{\phi}(\eta,s) = \frac{1}{s^2}e^{-\sqrt{s+a_1}\,\eta\sqrt{Sc}}, \tag{25}$$

$$\bar{\theta}(\eta,s) = \begin{cases} \frac{1}{s^2}e^{-\eta\sqrt{s\alpha}} + \frac{Du\alpha}{\alpha - Sc}\cdot\frac{sSc+K}{s^2(s-a_2)} \\ \times\left(e^{-\eta\sqrt{s\,Sc+K}} - e^{-\eta\sqrt{s\alpha}}\right) \text{for} \ \alpha \neq Sc, \\ \frac{1}{s^2}e^{-\eta\sqrt{sSc}} + \frac{Du\,Sc}{K}\cdot\frac{sSc+K}{s^2} \\ \times\left(e^{-\eta\sqrt{s\,Sc+K}} - e^{-\eta\sqrt{sSc}}\right)\text{for} \ \alpha = Sc, \end{cases} \tag{26}$$

$$\bar{u}_1(\eta,s) = \begin{cases} f(s)e^{-\eta\sqrt{s+c_1}} \\ +Gr\left\{\frac{1}{\alpha-1}\frac{1}{s^2(s-a_3)}\left(e^{-\eta\sqrt{s+c_1}} - e^{-\eta\sqrt{s\alpha}}\right)\right. \\ +\frac{Du\alpha}{\alpha-Sc}\frac{sSc+K}{s^2(s-a_2)}\left[\dfrac{e^{-\eta\sqrt{s+c_1}} - e^{-\eta\sqrt{sSc+K}}}{(Sc-1)(s-a_4)} \right. \\ \left. -\dfrac{e^{-\eta\sqrt{s+c_1}} - e^{-\eta\sqrt{s\alpha}}}{(\alpha-1)(s-a_3)}\right] \\ \left. +\frac{Gc}{s^2}\frac{e^{-\eta\sqrt{s+c_1}} - e^{-\eta\sqrt{sSc+K}}}{(Sc-1)(s-a_4)}\right\}\text{for} \ \alpha \neq Sc \neq 1, \\[3mm] f(s)e^{-\eta\sqrt{s+c_1}} + \frac{Gr}{Sc-1}\left\{\frac{1}{s^2(s-a_3)}\left(e^{-\eta\sqrt{s+c_1}} - e^{-\eta\sqrt{sSc}}\right)\right. \\ +\frac{Du\,Sc}{K}\frac{sSc+K}{s^2}\left[\dfrac{e^{-\eta\sqrt{s+c_1}} - e^{-\eta\sqrt{sSc+K}}}{s-a_4} \right. \\ \left. -\dfrac{e^{-\eta\sqrt{s+c_1}} - e^{-\eta\sqrt{sSc}}}{s-a_3}\right] \\ \left. +\frac{Gc}{Sc-1}\frac{e^{-\eta\sqrt{s+c_1}} - e^{-\eta\sqrt{sSc+K}}}{s^2(s-a_4)}\right\} \text{for} \ \alpha = Sc \neq 1 \end{cases} \tag{27}$$

where

$$\alpha = \frac{3R\,Pr}{3R+4}, \ c_1 = M^2 + \frac{1}{Da}, \ a_1 = \frac{K}{Sc},$$

$$a_2 = \frac{K}{\alpha - Sc}, \ a_3 = \frac{c_1}{\alpha - 1}, \ a_4 = \frac{c_1 - K}{Sc - 1}. \tag{28}$$

The inverse Laplace transforms of Eqs. (25) - (27) give the solutions for the concentration, temperature and velocity field distributions as

$$\phi(\eta,\tau) = F_1(\eta\sqrt{Sc},a_1,\tau), \tag{29}$$

$$\theta(\eta,\tau) =$$

$$\begin{cases} F_2(\eta\sqrt{\alpha},\tau) \\ +\frac{Du\,\alpha}{\alpha - Sc}\left[Sc\left\{F_3(\eta\sqrt{Sc},a_1,a_2,\tau) - F_4(\eta\sqrt{\alpha},a_2,\tau)\right\}\right. \\ \left. +K\left\{\begin{array}{l}F_5(\eta\sqrt{Sc},a_1,a_2,\tau) \\ -\frac{1}{a_2}\left(F_4(\eta\sqrt{\alpha},a_2,\tau) - F_2(\eta\sqrt{\alpha},\tau)\right)\end{array}\right\}\right]\text{for} \ \alpha \neq Sc, \\[5mm] F_2(\eta\sqrt{Sc},\tau) \\ -\frac{Du\,Sc}{K}\left[\begin{array}{l}Sc\left\{F_6(\eta\sqrt{Sc},a_1,\tau) - F_7(\eta\sqrt{Sc},\tau)\right\} \\ +K\left\{F_1(\eta\sqrt{Sc},a_1,\tau) - F_2(\eta\sqrt{Sc},\tau)\right\}\end{array}\right]\text{for} \ \alpha = Sc \end{cases} \tag{30}$$

$$u_1(\eta,\tau) =$$

$$\begin{cases} b_{ia} + Gr\left\{\frac{b_1 - b_2}{\alpha - 1} + \frac{Du\,\alpha}{\alpha - Sc}\left(Sc\left(\frac{b_3 - b_4}{Sc - 1} - \frac{b_5 - b_6}{\alpha - 1}\right)\right.\right. \\ \left.\left. K\left(\frac{b_7 - b_8}{Sc - 1} - \frac{b_9 - b_{10}}{\alpha - 1}\right)\right)\right\} + \frac{Gc}{Sc - 1}b_{11}\bigg]\text{for} \ \alpha \neq Sc \neq 1, \\[5mm] b_{ia} + \left[\frac{Gr}{Sc-1}\left\{\begin{array}{l}(b_1 - b_2) \\ -\frac{Du\,Sc}{K}\left(Sc(b_{12} - b_{13}) + K(b_{11} - b_{14})\right)\end{array}\right\}\right. \\ \left. +\frac{Gc}{Sc-1}b_{11}\right]\text{for} \ \alpha = Sc \neq 1 \end{cases} \tag{31}$$

where

$$b_{ia} = \begin{cases} F_6(\eta,c_1,\tau)\text{for impulsive motion of the plate} \\ F_1(\eta,c_1,\tau)\text{for accelerated motion of the plate} \end{cases}$$

and $b_1 - b_{14}$ and $F_1 - F_6$ are given in APPENDIX A.

2.1 Solution for Pure Convection

In the absence of thermal radiation, i.e. if pure convection prevails (corresponds to $R \to \infty$), it is observed that $\alpha = Pr$ and the solutions for the temperature and velocity given by (30) and (31) are valid for all values of $Pr \neq 1$ and $Sc \neq 1$. But the solution for velocity given by (31) is not valid for $Pr = 1$ or/and $Sc = 1$. Since the Prandtl number is a measure of the relative importance of the viscosity and thermal conductivity of the fluid, the case

$Pr = 1$ corresponds to those fluids whose momentum and thermal boundary layer thicknesses are of the same order of magnitude. Therefore, in the absence of thermal radiation effects the solution for the velocity field when $Pr = 1$ or/and $Sc = 1$ has to be obtained separately from Eqs. (16)-(18) subject to the initial and boundary conditions (19) and is given by

$$u_1(\eta, \tau) = \begin{cases} b_{ia} + \left[Gr \left\{ \dfrac{b_{15}}{c_1} + \dfrac{Du}{1-Sc} \left(Sc \left(\dfrac{b_3 - b_4}{Sc - 1} + \dfrac{b_{16}}{c_1} \right) \right. \right. \right. \\ \left. \left. + K \left(\dfrac{b_7 - b_8}{Sc - 1} + \dfrac{b_{17}}{c_1} \right) \right) \right\} + \dfrac{Gc}{Sc - 1} b_{11} \right] \text{ for } Pr = 1, \ Sc \neq 1 \\ b_{ia} + \left[Gr \left\{ \dfrac{b_{15}}{c_1} - \dfrac{Du}{K} \left(\left(\dfrac{b_{18}}{K - c_1} + \dfrac{b_{19}}{c_1} \right) \right. \right. \right. \\ \left. \left. K \left(\dfrac{b_{20}}{K - c_1} + \dfrac{b_{21}}{c_1} \right) \right) \right\} + \dfrac{Gc}{K - c_1} b_{20} \right] \text{ for } Pr = 1, \ Sc = 1 \end{cases}$$

(32)

where $a_2 = \dfrac{K}{1 - Sc}$

3. RESULTS AND DISCUSSION

To gain a perspective of the physics of the flow regime, we have presented the non-dimensional fluid velocity, fluid temperature and concentration, shear stress, the rate of heat and

mass transfers at the moving plate for several values of magnetic parameter M^2, Dufour number Du, thermal Grashof number Gr, mass Grashof number Gc, chemical reaction parameter K, porosity parameter Da, radiation parameter R, Prandtl number Pr, Schmidt number Sc and time τ either graphically

by MATLAB software or in tabular form for both the impulsive as well as the accelerated motion of the plate. Here we restrict our discussion to the aiding of favourable case only. To be realistic, the values of Schmidt number Sc are chosen for hydrogen $(Sc = 0.22)$, water vapour $(Sc = 0.6)$, ammonia $(Sc = 0.78)$ and Ethyl benzene $(Sc = 2.01)$ at temperature 25^0C and one atmospheric pressure. The values of thermal Grashof number Gr and mass Grashof number Gc are taken to be both positive and negative, which correspond to the cooling and heating of the plate respectively. Attention is focused on positive values of the buoyancy parameters i.e. Grashof number $Gr > 0$ (which corresponds to the cooling problem) and mass Grashof number $Gc > 0$ (which indicates that the chemical species concentration in the free stream region is less than the concentration at the boundary surface). The cooling problem is often encountered in engineering applications. For example in the cooling of electronic components and nuclear reactors. We take $R < 1$ (which means thermal conduction exceeds thermal radiation), $R > 1$ (which means thermal radiation exceeds

thermal conduction) and $R = 1$ (i.e. the contribution from both modes is equal) to get understand the effect of radiation on the temperature distribution and heat transfer rate at the plate.

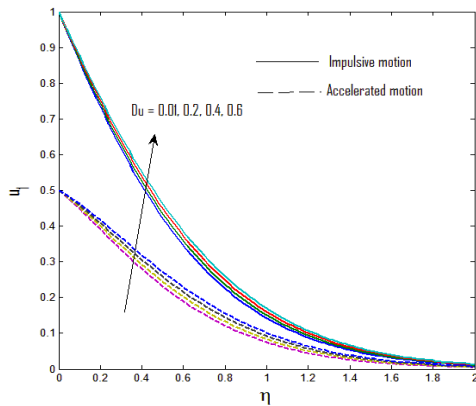### 3.1 Effects of Parameters on the Velocity Profiles

It is seen from Fig.2 that the fluid velocity u_1 decreases for both the impulsive as well as accelerated motion of the plate with an increase in magnetic parameter M^2. It is due to the presence of magnetic field normal to the flow in an electrically conducting fluid introduces a Lorentz force which acts against the flow and hence tends to reduce the fluid velocity. Increasing Lorentzian drag not only decelerates the flow in the boundary layer, it also arrests the flow more dramatically nearer the moving plate i.e. inhibits velocity development across the boundary layer transverse to the plate. The regulatory influence of a transverse magnetic field is therefore clearly identified and this result agrees strongly with numerous other studies in magnetohydrodynamic boundary layer flows. It is observed from Fig.3 that the fluid velocity u_1 increases for both the impulsive as well as accelerated motion of the plate with an increase in Dufour number Du. As the Dufour effect is more pronounced, the positive influence of concentration gradients on temperature field becomes higher so that the thermal boundary layer is enlarged which in tern increase the fluid velocity.
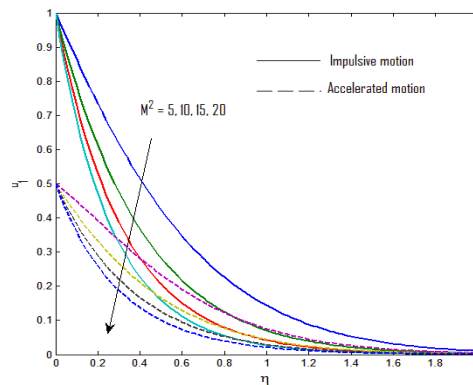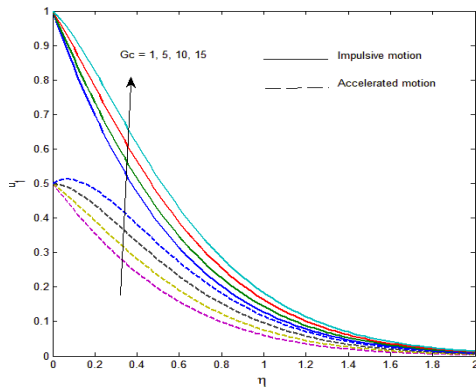

Fig. 2. Velocity profiles for M^2 when $Gr = 5$, $Gc = 5$, $Pr = 2$, $Sc = 0.22$, $Du = 0.03$, $K = 10$, $Da = 1$, $R = 10$ and $\tau = 0.5$.

It is seen from Fig.4 that the fluid velocity u_1 increases for both the impulsive as well as accelerated motion of the plate with an increase in mass Grashof number Gc. The mass Grashof number Gc defines the ratio of the species buoyancy force to the viscous hydrodynamic force. As expected, it is observed that there is a rise in the fluid velocity due to the enhancement of the species buoyancy force. It is observed from Fig.5 that the fluid velocity u_1 increases for both the impulsive as well as accelerated motion of the plate with an

increase in thermal Grashof number Gr . The thermal Grashof number Gr signifies the relative effect of the thermal buoyancy force to the viscous hydrodynamic force in the boundary layer. The fluid velocity increases due to the enhancement of the thermal buoyancy force. Therefore in materials processing systems in order to damp the flow near the moving plate, lower buoyancy forces are required. It is seen from Fig.6 that the fluid velocity u_1 decreases with an increase in chemical reaction parameter K for both the impulsive as well as accelerated motion of the plate. The hydrodynamics boundary layer becomes thin as the chemical reaction parameter increases which will cause slow down the fluid velocity.
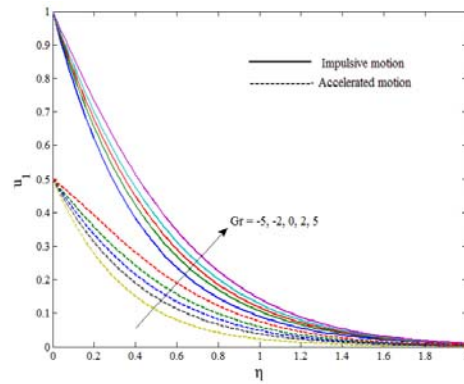
Schmidt number Sc for both the impulsive as well as accelerated motion of the plate. Schmidt number increases means the thickness of the concentration boundary layer decreases and this causes the velocity profile of the fluid decelerates.

Fig. 5. Velocity profiles for Gr **when** $Gc = 5$, $Du = 0.03$, $Pr = 2$, $Sc = 0.22$, $M^2 = 5$, $K = 10$, $Da = 1$, $R = 10$ **and** $\tau = 0.5$.

Fig. 3. Velocity profiles for Du **when** $Gr = 5$, $Gc = 5$, $Pr = 2$, $Sc = 0.22$, $M^2 = 5$, $K = 10$, $Da = 1$, $R = 10$ **and** $\tau = 0.5$.
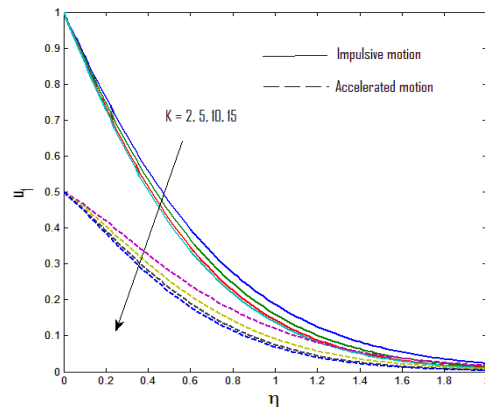

Fig. 6. Velocity profiles for K **when** $Gc = 5$, $Gr = 5$, $Du = 0.03$, $Sc = 0.22$, $M^2 = 5$, $Pr = 2$, $Da = 1$, $R = 10$ **and** $\tau = 0.5$.

Fig. 4. Velocity profiles for Gc **when** $Gr = 5$, $Du = 0.03$, $Pr = 2$, $Sc = 0.22$, $M^2 = 5$, $K = 10$, $Da = 1$, $R = 10$ **and** $\tau = 0.5$.

It is seen from Fig.7 that the fluid velocity u_1 increases with an increase in porosity parameter Da for both the impulsive as well as accelerated motion of the plate. For large porosity of the medium fluid gets more space to flow, as a consequence its velocity increases. Fig.8 shows that the fluid velocity u_1 decreases with an increase in
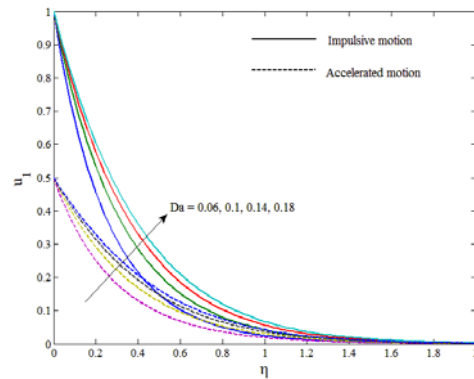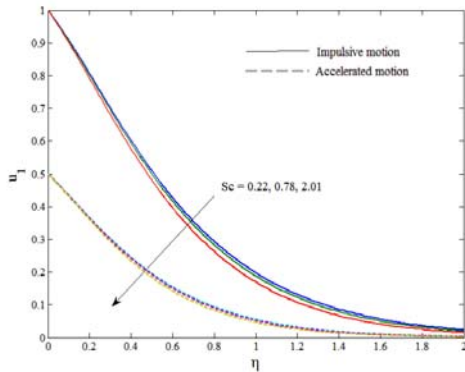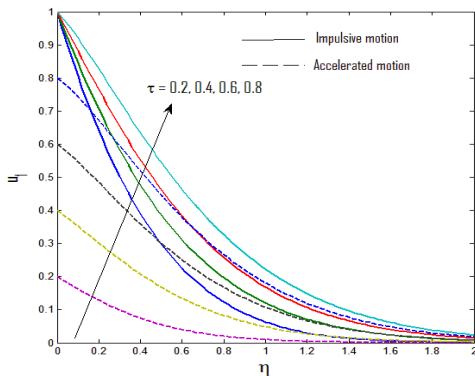

Fig. 7. Velocity profiles for Da **when** $Gc = 5$, $Gr = 5$, $Du = 0.03$, $Sc = 0.22$, $M^2 = 5$, $Pr = 2$, $K = 10$, $R = 10$ **and** $\tau = 0.5$.

It is seen from Fig.9 that the fluid velocity u_1 increases with an increase in time τ for both the impulsive as well as accelerated motion of the plate. This is due to increasing of buoyancy effects in the region as time progresses. The Figs.2-9 further establishes the fact that the fluid velocity decreases in a monotone fashion from the thin layer adjacent to the plate to zero asymptotically as $\eta \to \infty$. It is worth mentioning from Figs.2-9 that the fluid velocity is slightly greater in the case of impulsive motion than that of accelerated motion of the plate.

Fig. 8. Velocity profiles for Sc **when** $Gc = 5$, $Gr = 5$, $Du = 0.03$, $R = 10$, $M^2 = 5$, $Pr = 7$, $K = 10$, $Da = 1$ **and** $\tau = 0.5$.


Fig. 9. Velocity profiles for time τ **when** $Gc = 5$, $Gr = 5$, $Du = 0.03$, $R = 10$, $M^2 = 5$, $Pr = 2$, $K = 10$, $Da = 1$ **and** $Sc = 0.22$.

3.2 Effects of Parameters on the Temperature and Concentration Profiles

It is observed from Fig.10 that the fluid temperature θ decreases with an increase in radiation parameter R. This result qualitatively agrees with expectations, since the radiation causes a faster dissipation of heat and consequently lowers the temperature. This can be mathematically explained as a decrease in radiation parameter R for given k and T_∞ means a decrease in Rosseland radiation absorption coefficient k_R. Since divergence of the radiative heat flux $\frac{\partial q_r}{\partial y}$ increases, k_R decreases which in turn causes to increase the rate of radiative

heat transfer at the plate and hence the fluid temperature decreases. This means the thermal boundary layer decreases and more uniform temperature distributes across the boundary layer. Further, it is seen from Fig.10 that the fluid temperature θ decreases with an increase in Prandtl number Pr. The thermal conductivity of fluid decreases with an increase in Pr, resulting a decrease in thermal boundary layer thickness and the heat is able to diffuse away from the heated surface. Therefore, thermal diffusion has a tendency to reduce the fluid temperature. It is seen from Fig.11 that an increase in Dufour number Du leads to rise in the fluid temperature θ. The Dufour number is the ratio of concentration to temperature difference. Higher values of Dufour number Du imply a lower temperature difference, which results in an enhancement in the temperature profiles. As the Dufour number increases, concentration gradients therefore generally assist the flow and enhance thermal energy in the regime and also increase thermal boundary layer thickness. It is also observed from Fig.11 that an increase in chemical reaction parameter K leads to rise in the fluid temperature distribution θ. This can be attributed to internal heat generation in the fluid due to Arrhenius kinetics. It is observed from Fig.12 that both the temperature θ and concentration ϕ increase as time τ progresses. The chemical reaction reduces the local concentration, thus increasing its concentration gradient and its flux. As seen from the Fig.13, an increase in chemical reaction parameter K causes a decrease in the concentration of the chemical species in the boundary layer. Further, Fig.13 shows that the concentration ϕ decreases with an increase in Schmidt number Sc. Physically, it is true since increase of Sc means decrease of molecular diffusivity which results in decreasing of concentration boundary layer. Hence, the concentration of species is higher for small values of Sc. The profiles have the common feature that the fluid temperature and concentration distributions decrease in a monotone fashion from the surface to a zero value far away in the free stream.
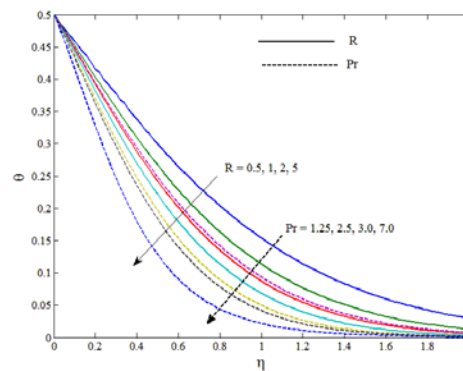

**Fig. 10. Temperature profiles for** R **and** Pr **when** $Du = 0.03$, $K = 10$, $\tau = 0.5$ **and** $Sc = 0.22$.

Table 1 The rate of mass transfer $\mathrm{Sh} = -\left(\dfrac{\partial \phi}{\partial \eta}\right)_{\eta=0}$ **at the moving plate** $\eta = 0$

	Sc				K			
τ	0.22	0.6	0.78	2.01	0.5	1	1.5	2
0.2	0.66724	0.72715	0.75515	0.93205	0.27102	0.30264	0.33200	0.35944
0.4	1.29969	1.35977	1.38821	1.57899	0.42800	0.50833	0.57934	0.64337
0.6	1.93215	1.99223	2.02069	2.21425	0.57504	0.70954	0.82460	0.92630
0.8	2.56460	2.62469	2.65315	2.84738	0.71889	0.90986	1.06960	1.20915
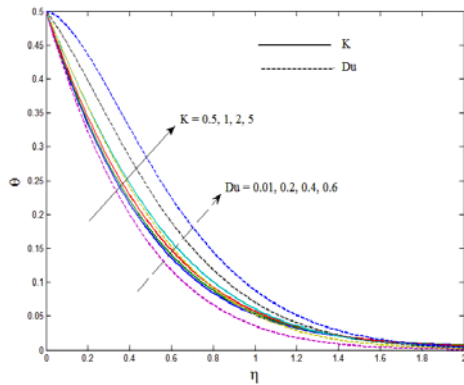
Fig. 11. Temperature profiles for K **and** Du **when** $\mathrm{R} = 10$, $\tau = 0.5$, $\mathrm{Pr} = 2$ **and** $\mathrm{Sc} = 0.22$.
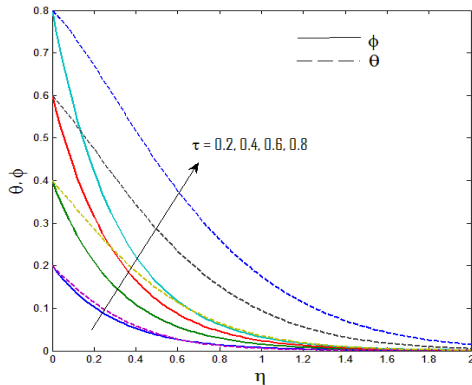
Fig. 12. Temperature and concentration profiles Du $= 0.03$, $\mathrm{Pr} = 2$, $K = 10$, $\mathrm{R} = 10$ **and** $\mathrm{Sc} = 0.22$.
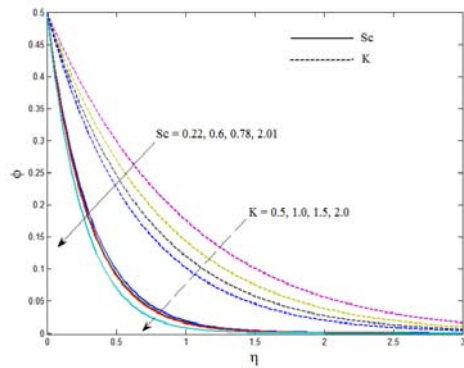
Fig. 13. Concentration profiles for Sc **and** K **when** $\tau = 0.5$.

3.3 Effects of Parameters on the Rate of Mass Transfer

The rate of mass transfer (Sherwood number) at the plate $\eta = 0$ is given by

$$\mathrm{Sh} = -\left(\frac{\partial \phi}{\partial \eta}\right)_{\eta=0} = \sqrt{\mathrm{Sc}}\, G_1(a_1, \tau). \qquad (33)$$

Numerical results of the rate of mass transfer at the plate $\eta = 0$ are presented in Table 1 for several values of Schmidt number Sc , chemical reaction parameter K and time τ . Table 1 shows that the rate of mass transfer increases with an increase in either Schmidt number Sc or chemical reaction parameter K . The variations of Schmidt number Sc as well as chemical reaction parameter K show that lesser the molecular diffusivity enhance the rate of mass transfer at the plate. With respect to time τ it is noticed that the rate of mass transfer increases in progressing of time. The effect of increase in time span is to enhance the rate of mass transfer at the plate.

3.4 Effects of Parameters on the Rate of Heat Transfer

The rate of heat transfer at the plate $\eta = 0$ is given by

$$\mathrm{Nu} = -\left(\frac{\partial \theta}{\partial \eta}\right)_{\eta=0}$$

$$= \begin{cases} \sqrt{\alpha}\, G_2(\tau) + \dfrac{\mathrm{Du}\,\alpha}{\alpha - \mathrm{Sc}}\Big[\mathrm{Sc}\big\{\sqrt{\mathrm{Sc}}\, G_3(a_1, a_2, \tau) - \sqrt{\alpha}\, G_4(a_2, \tau)\big\} \\ \quad + K\Big\{\sqrt{\mathrm{Sc}}\, G_5(a_1, a_2, \tau) - \dfrac{\sqrt{\alpha}}{a_2}\big(G_4(a_2, \tau) - G_2(\tau)\big)\Big\}\Big] \text{ for } \alpha \neq \mathrm{Sc} \\[2mm] \sqrt{\mathrm{Sc}}\Big[G_2(\tau) - \dfrac{\mathrm{Du}\,\mathrm{Sc}}{K}\big\{\mathrm{Sc}\big(G_6(a_1, \tau) - G_7(\tau)\big) \\ \quad + K\big(G_1(a_1, \tau) - G_2(\tau)\big)\big\}\Big] \qquad\qquad \text{for } \alpha = \mathrm{Sc} \end{cases}$$

$$(34)$$

Numerical results of the rate of heat transfer Nu at the wall $\eta = 0$ are presented in Table 2 for several values of Dufour number Du , chemical reaction parameter K , radiation parameter R and time τ . It is seen from Table 2 that the rate of heat transfer Nu increases with an increase in either radiation parameter R or time τ . In conclusion, it is very obvious from our results that thermal radiation intensifies the convective flow. Further, the rate of heat transfer Nu decreases with an increase in

Table 2 Rate of heat transfer $\mathrm{Nu} = -\left(\dfrac{\partial \theta}{\partial \eta}\right)_{\eta=0}$ **at the moving plate** $\eta = 0$

	Du			K			R		
τ	0.01	0.05	0.1	0.5	1	1.5	0.5	1	1.5
0.2	0.6646	0.6420	0.6137	0.6662	0.6654	0.6646	0.3658	0.4573	0.5076
0.4	0.9351	0.8837	0.8195	0.9410	0.9388	0.9367	0.5121	0.6390	0.7085
0.6	1.1403	1.0574	0.9537	1.1511	1.1472	1.1435	0.6145	0.7747	0.8583
0.8	1.3116	1.1955	1.0503	1.3276	1.3218	1.3164	0.7713	0.8868	0.9814

either Dufour number Du or chemical reaction parameter K. The effect of increase in time span is to enhance the rate of heat transfer at the plate. The negative sign indicates that the heat flows from the plate to fluid.

3.5 Effects of Parameters on the Shear Stress

From the engineering point of view, the most important characteristic of the flow is the shear stress at the plate $\eta = 0$ which is given by

$$\tau_x = \left(\frac{\partial u_1}{\partial \eta}\right)_{\eta=0}$$

$$= \begin{cases} m_{ia} + \left[\mathrm{Gr}\left\{\dfrac{m_1 - m_2}{\alpha - 1} + \dfrac{\mathrm{Du}\alpha}{\alpha - \mathrm{Sc}}\left(\mathrm{Sc}\left(\dfrac{m_3 - m_4}{\mathrm{Sc} - 1} - \dfrac{m_5 - m_6}{\alpha - 1}\right)\right.\right. \\ \left.\left. + K\left(\dfrac{m_7 - m_8}{\mathrm{Sc} - 1} - \dfrac{m_9 - m_{10}}{\alpha - 1}\right)\right)\right\} + + \dfrac{\mathrm{Gc}}{\mathrm{Sc} - 1}m_{11}\right] \text{ for } \alpha \neq \mathrm{Sc} \neq 1 \\[2em] m_{ia} + \left[\dfrac{\mathrm{Gr}}{\mathrm{Sc} - 1}\left\{m_1 - m_2 - \dfrac{\mathrm{Du}\alpha}{K}\left(\mathrm{Sc}\left(m_{12} - m_{13}\right)\right.\right.\right. \\ \left.\left.\left. + K\left(m_{11} - m_{14}\right)\right)\right\} + \dfrac{\mathrm{Gc}}{\mathrm{Sc} - 1}m_{11}\right] \text{ for } \alpha = \mathrm{Sc} = 1 \end{cases}$$

$$\tag{35}$$

where

$$m_{ia} = \begin{cases} G_6(c_1, \tau) & \text{for impulsive motion of the plate,} \\[1em] G_1(c_1, \tau) & \text{for accelerated motion of the plate} \end{cases}$$

and $m_1 - m_{14}$ and $G_1 - G_6$ are given in APPENDIX A.

The shear stress characterizes the frictional drag at the solid surface. Numerical values of the non-dimensional shear stress at the moving plate $\eta = 0$ are presented in Figs.14-17 for several values of magnetic parameter M^2, Dufour number Du, thermal Grashof number Gr and mass Grashof number Gc for both the impulsive as well as accelerated motion of the plate. Fig.14 shows that the magnitude of the shear stress τ_x at the plate increases with an increase in magnetic parameter M^2 for both the impulsive as well as accelerated motion of the plate. This suggests that greater Lorentz force with increasing acceleration of the plate gives an additional momentum in the boundary layer. The shear stresses are negative for

the large values of magnetic parameter M^2 which retard the flow in the boundary layer to such an extent that reversal of the flow is caused. This result is significant in the design of, for example, MHD generators since a critical magnetic flux density may be applied (i.e., magnetic parameter) to reverse the flow dynamics during operation. It is observed from Fig.15 that the magnitude of the shear stress τ_x at the plate decreases with an increase in Dufour number Du for both the impulsive as well as accelerated motion of the plate. This suggests that presence of Dufour effect reduces the frictional drag at the plate. It is observed from Figs.16 and 17 that the magnitude of the shear stress τ_x at the plate decreases with an increase in either thermal Grashof number Gr or mass Grashof number Gc for both the impulsive as well as accelerated motion of the plate. This means that the effects of buoyancy parameters also decelerate the frictional drag at the plate. We note that values become negative for very low values of either Gr or Gc since the magnetic impedance force $M^2 = 5$ will dominate and have a greater inhibiting influence with low buoyancy that is, flow reversal accompanies lower thermal buoyancy forces for higher permeability regimes. On careful observation, it is revealed from Figs.14-17 that the shear stress near the plate is negative as time progresses. Thus, it may be concluded that time span plays an important role to modify the frictional drag due to shear stress at the plate.
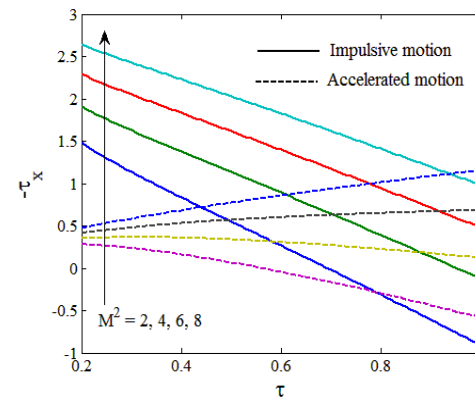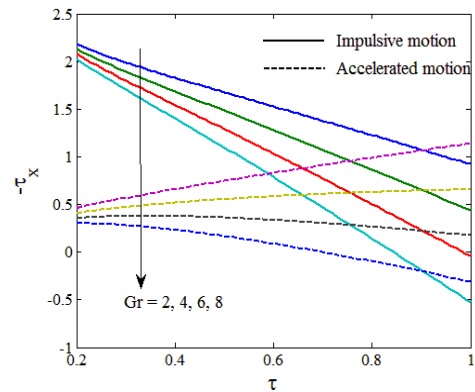

Fig. 14. Shear stress $-\tau_x$ **for** M^2 **when** $\mathrm{Gc} = 5$, $\mathrm{Gr} = 5$, $\mathrm{Pr} = 2$, $K = 10$, $R = 10$, $\mathrm{Da} = 1$, $\mathrm{Du} = 0.03$ **and** $\mathrm{Sc} = 0.22$.
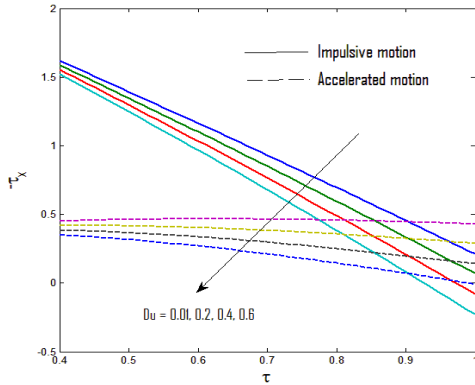
Fig. 15. Shear stress $-\tau_x$ **for** Du **when** $Gc = 5$, $Gr = 5$, $Du = 0.03$, $Pr = 2$, $K = 10$, $R = 10$, $Da = 1$, **and** $Sc = 0.22$.
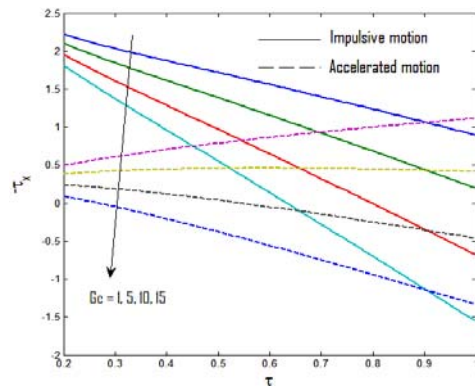
Fig. 16. Shear stress $-\tau_x$ **for** Gc **when** $Gr = 5$, $R = 10$, $M^2 = 5$, $Pr = 2$, $K = 10$, $Da = 1$, $Du = 0.03$ **and** $Sc = 0.22$.

Fig. 17. Shear stress $-\tau_x$ **for** Gr **when** $Gc = 5$, $R = 10$, $M^2 = 5$, $Pr = 2$, $K = 10$, $Da = 1$, $Du = 0.03$ **and** $Sc = 0.22$.

In the absence of thermal radiation, i.e. if pure convection prevails (corresponds to $R \to \infty$), the solutions for the rate of heat transfer and shear stress at the plate given by (34) and (35) are valid for all values of $Pr \neq 1$ and $Sc \neq 1$. But the solution for shear stress at the plate given by (35) is not valid

for $Pr = 1$ or/and $Sc = 1$. In the absence of thermal radiation effects the solution for the shear stress at the plate when $Pr = 1$ or/and $Sc = 1$ is given by

$$\tau_x = \left(\frac{\partial u_1}{\partial \eta}\right)_{\eta=0}$$

$$= \begin{cases} m_{ia} + \left[Gr\left\{\frac{m_{15}}{c_1} + \frac{Du}{1-Sc}\left(Sc\left(\frac{m_3 - m_4}{Sc-1} + \frac{m_{16}}{c_1}\right)\right.\right. \\ \left.\left. + K\left(\frac{m_7 - m_8}{Sc-1} + \frac{m_{17}}{c_1}\right)\right)\right\} + \frac{Gc}{Sc-1}m_{11}\right] \text{for } Pr=1, \ Sc \neq 1 \\ \\ m_{ia} + \left[Gr\left\{\frac{m_{15}}{c_1} - \frac{Du}{K}\left(Sc\left(\frac{m_{18}}{K-c_1} + \frac{m_{19}}{c_1}\right)\right.\right.\right. \\ \left.\left. + K\left(\frac{m_{20}}{K-c_1} + \frac{m_{21}}{c_1}\right)\right)\right\} + \frac{Gc}{K-c_1}m_{20}\right] \text{for } Pr=1, \ Sc=1 \end{cases}$$

(36)

where $a_2 = \dfrac{K}{1-Sc}$.

4. CONCLUSION

The purpose of this study is to analyze the effects of diffusion-thermo and thermal radiation on an unsteady magnetohydrodynamic free convective boundary layer flow of a viscous incompressible electrically conducting fluid past a moving infinite vertical plate in the presence of a transverse uniform magnetic field. Rosseland diffusion approximation is used to describe the radiative heat flux in the energy equation. The expressions for the velocity and the temperature have been obtained in closed form with the help of the Laplace transform technique. The effects of the pertinent parameters on velocity, temperature and concentration profiles are presented graphically. The influences of the same parameters on the shear stress and rates of heat and mass transfer at the plate are also discussed in details. The most important concluding remarks can be summarized as follows:

• Magnetic field has a retarding influence whereas porosity of the medium has an accelerating influence on the fluid velocity for both the impulsive as well as accelerated motion of the plate.

• Either Dufour number or mass Grashof number or thermal Grashof number has an accelerating influence on the fluid velocity whereas they have a retarding influence on the absolute value of the shear stress at the plate for both cases

of the impulsive as well as accelerated motion of the plate.

• Thermal radiation has a retarding influence on the fluid temperature.

• Increasing Dufour number heats the regime, i.e. boosts temperature.

• Chemical reaction parameter has a retarding influence on the concentration distribution whereas it tends to enhance the rate of mass

transfer at the plate.

• The fluid velocity, temperature and concentration distributions, the rates of heat and mass transfer increase as time progresses.

• The growths of both the momentum and temperature boundary layer thicknesses are also shown to be elevated by Dufour effects.

REFERENCES

Ahamed, S. and J. Zueco (2010). Combined heat and mass transfer by mixed convection MHD flow along a porous plate with chemical reaction in presence of heat source. *Appl. Math. Mech.* 31(10), 1217-1230.

Ahmed, N. (2012). Soret and radiation effects on transient MHD free convection from an impulsively started infinite vertical plate. *J. Heat Transfer* 134, 062701-1.

Ahmed, N. and H. K. Sarmah (2009). Thermal radiation effect on a transient MHD flow with mass transfer past an impulsively fixed infinite vertical plate. *Int. J. Appl. Math. Mech.* 5(5), 87-98.

Alam, M. S. and M. M. Rahman (2006). Dufour and Soret effects on mixed convection flow past a vertical porous flat plate with variable suction. *Nonlinear Anal. Model. Control* 11, 3–12.

Alam, M. S., M. Ferdows, M. Ota and M. A. Maleque (2006b). Dufour and Soret effects on steady free convection and mass transfer flow past a semi-infinite vertical porous plate in a porous medium. *Int. J. Appl. Mech. Eng.* 11(3), 535-545.

Alam, M. S., M. M. Rahman and M. A. Smad (2006a). Dufour and Soret effects on unsteady MHD free convection and mass transfer flow past a vertical porous plate in a porous medium, *Nonlinear Analy. Model. Control* 11(3), 217-226.

Alam, M. S., M. M. Rahman, M. Ferdows, K.. Kaino, E. Mureithi and A. Postelnicu (2007). Diffusion-thermo and thermal-diffusion effects on free convective heat and mass transfer flow on a porous medium with time dependent temperature and concentration. *Int. J. Appl. Eng. Research* 2(1), 81-96.

Chandrakala, P. and N. Bhaskar (2014). Radiation effects on MHD flow past an impulsively started infinite vertical plate with mass diffusion. *Int. J. Appl. Mech. Eng.* 19(1), 17-26.

Cramer, K. R. and S. I. Pai (1973). Magnetofluid dynamics for engineers and applied physicists. *McGraw-Hill, New York.*

Das, S., M. Jana and R. N. Jana (2011). Radiation effect on natural convection near a vertical plate embedded in porous medium with ramped wall temperature. *Open J.Fluid Dynamics* 1, 1-11.

Das, U. N., R. K. Deka and V. M. Soundalgekar (1996). Radiation effects on flow past an impulsively started vertical infinite plate. *J. Theoretical Mech.* 1, 111-115.

Gupta, A. S., I. Pop and V. M. Soudalgekar (1979). Free convection effects on the flow past an accelerated vertical plate in an incompressible dissipative fluid. *Roum. Sci. Techn. Mech. Appl.* 24, 561-568.

Hossain, M. A. and H. S. Takhar (1996). Radiation effect on mixed convection along a vertical plate with uniform surface temperature. *Heat and Mass Transfer* 31, 243-248.

Hossain, M. A. and L. K.. Shayo (1986). The Skin friction in the unsteady free convection flow past an accelerated plate. *Astrophys. Space Sci.* 125, 315-324.

Ibrahim, S. M., K. Gangadhar and N. Bhaskar Reddy (2015). Radiation and mass transfer effects on MHD oscillatory flow in a channel filled with porous medium in the presence of chemical reaction. *J. Appl. Fluid Mech.* 8(3), 529-537.

Jana, M., S. Das and R. N. Jana (2012). Radiation effects on unsteady MHD free convective flow past an exponentially accelerated vertical plate with viscous and Joule dissipations. *Int. J. Eng. Research Appl.* 2(5), 270-278.

Jana, R. N. and N. Datta (1982). Unsteady free convective flow past a moving vertical plate. *Mathematical Forum* 5, 14-20.

Jha, B. K. and A. O. Ajibade (2009). Diffusion-thermo effects on free convective heat and mass transfer flow in a vertical channel with symmetric boundary conditions. *J. Heat Transfer* 133, 1-8

Kafoussias, N. G. (1992). MHD thermal-diffusion effects on free convective and mass transfer flow over an infinite vertical moving plate. *Astrophys. Space Sci.* 192(1), 11-19.

Kishore, P. M., N. V. R. V. Prasada Rao, S. V. K. Varma and S. Venkataramana (2013). The effects of radiation and chemical reaction on unsteady MHD free convection flow of viscous fluid past an exponentially accelerated vertical plate. *Int. J. Phys. Math. Sci.* 4(1), 300-317.

Makinde, O. D. (2010). On MHD heat and mass transfer over a moving vertical plate with a convective surface boundary condition. *The Canadian J. Chem. Eng.* 88, 983-990.

Makinde, O. D. (2011). MHD mixed-convection interaction with thermal radiation and nth order chemical reaction past a vertical porous plate embedded in a porous medium. *Chem. Eng.. Comm.* 198, 590–608.

Makinde, O. D. (2012). Chemically reacting hydromagnetic unsteady flow of a radiating fluid past a vertical plate with constant heat flux. Z. Naturforsch 67, 239–247.

Mandal, C., S. L. Maji, S. Das and R. N. Jana (2011). Effects of radiation and heat transfer on

flow past an exponentially accelerated vertical plate with constant heat flux. *Advances in Theo. Appl. Math*. 6(5), 579-590.

Manna, G., S. L., Maji, M. Guria and R. N. Jana (2007). Unsteady viscous flow past a flat plate in a rotating system. *J. Phys. Sci.* 11, 29-42.

Muthucumaraswamy, R. and A. Vijayalakshmi (2005). Radiation effects on flow past an impulsively started vertical plate with variable temperature and mass flux. *Theoreical Appl. Mech*. 32(3), 223-234.

Muthucumaraswamy, R., M. Sundar Raj and V. S. A. Subramanian (2009). Unsteady flow past an accelerated infinite vertical plate with variable temperature and uniform mass diffusion. *Int. J. Appl. Math. Mech*. 5(6), 51-56.

Muthucumaraswamy, R., M. Sundar Raj and V. S. A. Subramanian (2009). Heat and mass transfer effects on flow past an accelerated vertical plate with variable mass diffusion. *Int. J. Appl. Math. Eng. Sci.* 3(1), 55-60.

Pattnaik, J. R., G. C. Dash and S. Singh (2012). Radiation and mass transfer effects on MHD free convection flow through porous medium past an exponentially accelerated vertical plate with variable temperature. *Int. J. Eng. Tome X*, 175-182.

Prakash, J., D. Bhanumathi, A. G. K. Vijaya and S. V. K., Varma (2013). Diffusion-thermo and radiation effects on unsteady MHD flow through porous medium past an impulsively started infinite vertical plate with variable temperature and mass diffusion, *Transp. Porous Media* 96, 135-151.

Rajesh, V. and S. V. K. Varma (2009). Radiation and mass transfer effects on MHD free convection flow past an exponentially accelerated vertical plate with variable temperature. *ARPN J. Eng. Appl. Sci.* 4(6), 20-26.

Rajesh, V. and S. V. K. Varma (2010). Radiation effects on MHD flow through a porous medium with variable temperature or variable mass diffusion. *Int. J. Appl. Math. Mech.* 6(1), 39-57.

Rajput, U. S. and S. Kumar (2012). Radiation effects on MHD flow past an impulsively started vertical plate with variable heat and mass transfer. *Int. J. Appl. Math. Mech*. 8(1), 66-85.

Raptis, A. and C. Perdikis (1999). Radiation and free convection flow past a moving plate. *Int. J. Appl. Mech. Eng.* 4, 817-821.

Seethamahalakshmi, G. V. Ramana Reddy and B. D. C. N. Prasad (2011). Unsteady effects of thermal radiation on MHD free convection flow past a vertical porous plate. *J. Comp. Math. Sci.* 2(4), 595-604.

Siegel, R. and J. R. Howell (2002). Thermal radiation heat transfer, *Taylor and Francis, New York*.

Singh, A. K. and N. Kumar (1984). Free convection flow past an exponentially accelerated vertical plate. *Astrophys. Space Sci*. 98, 245-258.

Suneetha, S. and N. Bhaskar Reddy (2011). Radiation and darcy effects on unsteady MHD heat and mass transfer flow of a chemically reacting fluid past an impulsively started vertical plate with heat generation. *Int. J. Appl. Math. Mech.* 7(7), 1-19.

Vijaya, A. G. K. and S. V. K. Verma (2011). Radiation effects on MHD flow past an impulsively started exponentially accelerated vertical plate with variable temperature in the presence of heat generation. *Int. J. Eng. Sci. Tech.* 3(4), 2898-2909.

Yasmin, D., T. Ahmed, N. N. Anika, M. M. M. Hasan and M. M. Alam (2014). Diffusion-Thermo and Thermal-diffusion effects on MHD visco-elastic fluid flow over a vertical plate. *J. Appl. Fluid Mech.* 7(3), 447-458.

APPENDIX A

$$b_1 = F_5(\eta, c_1, a_3, \tau),$$

$$b_2 = \frac{1}{a_3}\Big[F_4(\eta\sqrt{\alpha}, a_3, \tau) - F_2\big(\eta\sqrt{\alpha}, \tau\big)\Big],$$

$$b_3 = \frac{1}{a_2 - a_4}\Big[F_3(\eta, c_1, a_2, \tau) - F_3(\eta, c_1, a_4, \tau)\Big],$$

$$b_4 = \frac{1}{a_2 - a_4}\Big[F_3(\eta\sqrt{Sc}, a_1, a_2, \tau) - F_3\big(\eta\sqrt{Sc}, a_1, a_4, \tau\big)\Big],$$

$$b_5 = \frac{1}{a_2 - a_3}\Big[F_3(\eta, c_1, a_2, \tau) - F_3(\eta, c_1, a_3, \tau)\Big],$$

$$b_6 = \frac{1}{a_2 - a_3}\Big[F_4(\eta\sqrt{\alpha}, a_2, \tau) - F_4\big(\eta\sqrt{\alpha}, a_3, \tau\big)\Big],$$

$$b_7 = \frac{1}{a_2 - a_4}\Big[F_5(\eta, c_1, a_2, \tau) - F_5(\eta, c_1, a_4, \tau)\Big],$$

$$b_8 = \frac{1}{a_2 - a_4}\Big[F_5(\eta\sqrt{Sc}, a_1, a_2, \tau) - F_5\big(\eta\sqrt{Sc}, a_1, a_4, \tau\big)\Big],$$

$$b_9 = \frac{1}{a_2 - a_3}\Big[F_5(\eta, c_1, a_2, \tau) - F_5\big(\eta, c_1, a_3, \tau\big)\Big],$$

$$b_{10} = \frac{1}{a_2 - a_3}\Big[\frac{1}{a_2}(F_4(\eta\sqrt{\alpha}, a_2, \tau) - F_2(\eta\sqrt{\alpha}, \tau)) $$
$$ - \frac{1}{a_3}(F_4(\eta\sqrt{\alpha}, a_3, \tau) - F_2(\eta\sqrt{\alpha}, \tau))\Big],$$

$$b_{11} = F_5(\eta, c_1, a_4, \tau) - F_5(\eta\sqrt{Sc}, a_1, a_4, \tau),$$

$$b_{12} = F_3(\eta, c_1, a_4, \tau) - F_3(\eta\sqrt{Sc}, a_1, a_4, \tau),$$

$$b_{13} = F_3(\eta, c_1, a_3, \tau) - F_4(\eta\sqrt{Sc}, a_3, \tau),$$

$b_{14} = F_5(\eta, c_1, a_3, \tau) - \dfrac{1}{a_3}(F_4(\eta\sqrt{Sc}, a_3, \tau) - F_2(\eta\sqrt{Sc}, \tau)),$

$b_{15} = F_2(\eta, \tau) - F_1(\eta, c_1, \tau),$

$b_{16} = F_3(\eta, c_1, a_2, \tau) - F_4\left(\eta, a_2, \tau\right),$

$b_{17} = F_5(\eta, c_1, a_2, \tau) - \dfrac{1}{a_4}\left(F_4\left(\eta, a_2, \tau\right) - F_2(\eta, \tau)\right),$

$b_{18} = F_6(\eta, c_1, \tau) - F_6\left(\eta, K, \tau\right),$

$b_{19} = F_6(\eta, c_1, \tau) - F_7\left(\eta, \tau\right),$

$b_{20} = F_1(\eta, c_1, \tau) - F_1\left(\eta, K, \tau\right),$

$b_{21} = F_6(\eta, c_1, \tau) - F_2\left(\eta, \tau\right),$

$F_1(\xi, y, \tau) = \left(\dfrac{\tau}{2} + \dfrac{\xi}{4\sqrt{y}}\right)e^{\xi\sqrt{y}}\text{erfc}\left(\dfrac{\xi}{2\sqrt{\tau}} + \sqrt{y\tau}\right)$

$+ \left(\dfrac{\tau}{2} - \dfrac{\xi}{4\sqrt{y}}\right)e^{-\xi\sqrt{y}}\text{erfc}\left(\dfrac{\xi}{2\sqrt{\tau}} - \sqrt{y\tau}\right),$

$F_2(\xi, \tau) = \dfrac{1}{2}\left(2\tau + \xi^2\right)\text{erfc}\left(\dfrac{\xi}{2\sqrt{\tau}}\right) - \xi\sqrt{\dfrac{\tau}{\pi}}e^{-\frac{\xi^2}{4\tau}},$

$F_3(\xi, y, z, \tau) = \dfrac{1}{z}\left[\dfrac{1}{2}e^{z\tau}\left\{e^{\xi\sqrt{y+z}}\text{erfc}\left(\dfrac{\xi}{2\sqrt{\tau}} + \sqrt{(y+z)\tau}\right)\right.\right.$

$\left. + e^{-\xi\sqrt{y+z}}\text{erfc}\left(\dfrac{\xi}{2\sqrt{\tau}} - \sqrt{(y+z)\tau}\right)\right\}$

$\left. - \dfrac{1}{2}\left\{e^{\xi\sqrt{y}}\text{erfc}\left(\dfrac{\xi}{2\sqrt{\tau}} + \sqrt{y\tau}\right) + e^{-\xi\sqrt{y}}\text{erfc}\left(\dfrac{\xi}{2\sqrt{\tau}} - \sqrt{y\tau}\right)\right\}\right],$

$F_4(\xi, y, \tau) = \dfrac{1}{y}\left[\dfrac{1}{2}e^{y\tau}\left\{\begin{array}{l}e^{\xi\sqrt{y}}\text{erfc}\left(\dfrac{\xi}{2\sqrt{\tau}} + \sqrt{y\tau}\right)\\[2mm] + e^{-\xi\sqrt{y}}\text{erfc}\left(\dfrac{\xi}{2\sqrt{\tau}} - \sqrt{y\tau}\right)\end{array}\right\}\right.$

$\left. - \text{erfc}\left(\dfrac{\xi}{2\sqrt{\tau}}\right)\right],$

$F_5(\xi, y, z, \tau) = \dfrac{1}{z}\left[\dfrac{1}{2z}e^{z\tau}\left\{e^{\xi\sqrt{y+z}}\text{erfc}\left(\dfrac{\xi}{2\sqrt{\tau}} + \sqrt{(y+z)\tau}\right)\right.\right.$

$\left. + e^{-\xi\sqrt{y+z}}\text{erfc}\left(\dfrac{\xi}{2\sqrt{\tau}} - \sqrt{(y+z)\tau}\right)\right\}$

$- \left(\dfrac{\tau}{2} + \dfrac{\xi}{4\sqrt{y}} + \dfrac{1}{2z}\right)e^{\xi\sqrt{y}}\text{erfc}\left(\dfrac{\xi}{2\sqrt{\tau}} + \sqrt{y\tau}\right)$

$\left. - \left(\dfrac{\tau}{2} - \dfrac{\xi}{4\sqrt{y}} + \dfrac{1}{2z}\right)e^{-\xi\sqrt{y}}\text{erfc}\left(\dfrac{\xi}{2\sqrt{\tau}} - \sqrt{y\tau}\right)\right],$

$F_6(\xi, y, \tau)$

$= \dfrac{1}{2}\left[e^{\xi\sqrt{y}}\text{erfc}\left(\dfrac{\xi}{2\sqrt{\tau}} + \sqrt{y\tau}\right) + e^{-\xi\sqrt{y}}\text{erfc}\left(\dfrac{\xi}{2\sqrt{\tau}} - \sqrt{y\tau}\right)\right],$

$F_7(\xi, \tau) = \text{erfc}\left(\dfrac{\xi}{2\sqrt{\tau}}\right),$

$m_1 = G_5(c_1, a_3, \tau), \quad m_2 = \dfrac{\sqrt{\alpha}}{a_3}\left[G_4(a_3, \tau) - G_2\left(\tau\right)\right],$

$m_3 = \dfrac{1}{a_2 - a_4}\left[G_3(c_1, a_2, \tau) - G_3\left(c_1, a_4, \tau\right)\right],$

$m_4 = \dfrac{\sqrt{Sc}}{a_2 - a_4}\left[G_3(a_1, a_2, \tau) - G_3\left(a_1, a_4, \tau\right)\right],$

$m_5 = \dfrac{1}{a_2 - a_3}\left[G_3(c_1, a_2, \tau) - G_3\left(c_1, a_3, \tau\right)\right],$

$m_6 = \dfrac{\sqrt{\alpha}}{a_2 - a_3}\left[G_4(a_2, \tau) - G_4\left(a_3, \tau\right)\right],$

$m_7 = \dfrac{1}{a_2 - a_4}\left[G_5(c_1, a_2, \tau) - G_5\left(c_1, a_4, \tau\right)\right],$

$m_8 = \dfrac{\sqrt{Sc}}{a_2 - a_4}\left[G_5(a_1, a_2, \tau) - G_5\left(a_1, a_4, \tau\right)\right],$

$m_9 = \dfrac{1}{a_2 - a_3}\left[G_5(c_1, a_2, \tau) - G_5\left(c_1, a_3, \tau\right)\right],$

$m_{10} = \dfrac{\sqrt{\alpha}}{a_2 - a_3}\left[\begin{array}{l}\dfrac{1}{a_2}(G_4(a_2, \tau) - G_2(\tau))\\[2mm] - \dfrac{1}{a_3}(G_4(a_3, \tau) - G_2(\tau))\end{array}\right],$

$m_{11} = G_5(c_1, a_4, \tau) - \sqrt{Sc}\,G_5(a_1, a_4, \tau),$

$m_{12} = G_3(c_1, a_4, \tau) - \sqrt{Sc}\,G_3(a_1, a_4, \tau),$

$m_{13} = G_3(c_1, a_3, \tau) - \sqrt{Sc}\,G_4(a_3, \tau),$

$m_{14} = G_5(c_1, a_3, \tau) - \dfrac{\sqrt{Sc}}{a_3}(G_4(a_3, \tau) - G_2(\tau)),$

$m_{15} = G_2(\tau) - G_1(c_1, \tau),$

$m_{16} = G_3(c_1, a_2, \tau) - G_4\left(a_2, \tau\right),$

$m_{17} = G_5(c_1, a_2, \tau) - \dfrac{1}{a_4}\left(G_4\left(a_2, \tau\right) - G_2(\tau)\right),$

$m_{18} = G_6(c_1, \tau) - G_6\left(K, \tau\right), \quad m_{19} = G_6(c_1, \tau) - G_7\left(\tau\right),$

$m_{20} = G_1(c_1, \tau) - G_1\left(K, \tau\right), \quad m_{21} = G_6(c_1, \tau) - G_2\left(\tau\right),$

$G_1(\xi, \tau) = 2\left(\dfrac{1}{4\sqrt{\xi}} + \dfrac{\tau}{2}\sqrt{\xi}\right)\text{erf}(\sqrt{\xi\tau}) + \sqrt{\dfrac{\tau}{\pi}}e^{-\xi\tau},$

$G_2(\tau) = -2\sqrt{\dfrac{\tau}{\pi}},$

$G_3(\xi, y, \tau)$

$= -\dfrac{1}{y}\left[e^{y\tau}\left\{\sqrt{\xi + y}\,\text{erf}\left(\sqrt{(\xi+y)\tau}\right) + \dfrac{1}{\sqrt{\pi\tau}}e^{-(\xi+y)\tau}\right\}\right.$

$\left. - \left\{\sqrt{\xi}\,\text{erf}\left(\sqrt{\xi\tau}\right) + \dfrac{1}{\sqrt{\pi\tau}}\,e^{-\xi\tau}\right\}\right],$

$G_4(\xi, \tau) = -\dfrac{1}{\xi}e^{\xi\tau}\sqrt{\xi}\,\text{erf}\left(\sqrt{\xi\tau}\right),$

$G_5(\xi, y, \tau)$

$$= -\frac{1}{y}\left[\frac{1}{y}e^{y\tau}\left\{\sqrt{\xi+y}\ \mathrm{erf}\left(\sqrt{(\xi+y)\tau}\right)+\frac{1}{\sqrt{\pi\tau}}e^{-(\xi+y)\tau}\right\}\right.$$

$$\left.-\left(\tau+\frac{1}{2\xi}+\frac{1}{y}\right)\sqrt{\xi}\ \mathrm{erf}\left(\sqrt{\xi\tau}\right)-\left(\tau+\frac{1}{y}\right)\frac{1}{\sqrt{\pi\tau}}e^{-\xi\tau}\right],$$

$$G_6(\xi, \tau) = -\left[\sqrt{\xi}\ \mathrm{erf}\left(\sqrt{\xi\tau}\right)+\frac{1}{\sqrt{\pi\tau}}e^{-\xi\tau}\right],$$

$$G_7(\tau) = -\frac{1}{\sqrt{\pi\tau}},$$

where erf (.) is the error function and erfc (.) the complementary error function. ξ, y, z are dummy variables.